EFFECT OF THE NON-CONDENSABLE GAS TYPE DURING CONDENSATION OF WATER VAPOR

by

Kaoutar ZINE-DINE*, Youness EL HAMMAMI, Rachid MIR, Touria MEDIOUNI, and Sara ARMOU

Laboratory of Mechanics, Process, Energy, and Environment,
Ibn Zohr University, ENSA, Agadir, Morocco

Original scientific paper
https://doi.org/10.2298/TSCI160612294Z

In this paper, a numerical study is performed to investigate the influence of the non-condensable gas type in a vapor mixture of water gas (water vapor-krypton, water vapor-argon, water vapor-air, and water vapor-neon) during the condensation along a vertical pipe with a wall cooled by air-flow. The applied numerical method solves the coupled parabolic governing equations in both gas and liquid phases with the appropriate boundary and interfacial conditions. The equations systems, obtained by using an implicit finite difference method are solved by Thomas algorithm. The numerical results obtained show that the heat and mass transfer is influenced by increasing the molar mass of non-condensable gases. The comparisons of air mass fraction, bulk temperature, local condensate heat transfer coefficient, and average Nusselt number of sensible heat with the literature results and the available experimental data are in good agreement.

Key words: *condensation, non-condensable gas, phase change, heat and mass transfer, molar mass*

Introduction

Gas-liquid flow systems with coupled heat and mass transfer during condensation in a vertical tube are encountered in many industrial processes such as: refrigeration engineering, heat exchangers and chemical processing and also nuclear reactors, where the condensation of steam is used for cooling the walls. For this reason, the film condensation topic has been studied since the beginning of the 19th century. Hence, Nusselt [1] analyzed the film condensation on a vertical surface, considering the local balance between the viscous forces and the weight of the condensate film. His results showed that the heat transfer in condensation depend on the local thickness of the film. Rohsenow [2] makes a change to the Nusselt theory considering convection enthalpy in the condensate liquid film and considers that the temperature profile is no longer linear. In fact, condensation process of water vapor from the vapor-gas mixtures with non-condensable gas is more complex than that corresponding to pure vapor and constitutes an important phenomenon in the cooling systems and because of its build up at the liquid mixture interface. Siddiqui *et al.* [3] has conducted an experimental study of the forced convection inducted by condensation of two types of mixtures: steam-air and steam water-helium on the inside wall of a vertical tube. They have found that for the same mass fraction of non-condensable gas,

* Corresponding author, e-mail: zinedinekaouthar@gmail.com

helium has more effect than the air on reducing the heat transfer. The same authors, Siddiqui *et al.* [4] have also performed a theoretical study of the condensation by forced convection of a mixture steam-gas in a vertical tube, considering different gases (air, hydrogen, helium). They have shown that the presence of air, hydrogen or helium, respectively, leads to condensation rate increasingly higher. Merouani *et al.* [5] have presented a numerical modeling of the convective condensation of a mixture of steam in the presence of a non-condensable gas (argon, air, helium, hydrogen) between two vertical coaxial cylinders. They have concluded that the heaviest mixture (vapor-argon) has the lower mass fraction of steam in the outlet and therefore, the highest thickness of the liquid film, the rate of condensation and the mass flow of liquid.

The influence of steam Reynolds number have been analyzed numerically by Maheshwari *et al.* [6] during the condensation of a vapor mixture of water and non-condensable gas inside a tube. They have shown that for low inlet Reynolds numbers, the thermal resistance of non-condensable gas layer in the vapor-condensate interface is higher than that of the condensate film. An experimental investigation of the condensation of steam and mixtures of non-condensable gas inside a vertical tube immersed in a water reservoir has been introduced by Oh and Revankar [7] in order to analyze the influence of vapor pressure on the condensation. The results show that the heat transfer coefficient and the heat flow density towards the wall decreases with the increase of air mass fraction. In addition, the heat flow transferred to the wall decreases when the vapor pressure increases, while the heat flow density on the wall increases with the pressure enhancement. Saffari and Dalir [8] analyzed the effect of virtual mass force on prediction of pressure changes in condensing tubes. They have used three-fluid model to calculate the pressure drops in a vertical pipe with the annular flow pattern for condensing steam. The 3-D models are based on the mass, momentum, and energy balance equations for each of the fluid streams in the annular flow.

El Hammami *et al.* [9] have modelled film condensation from a steam-air mixture with small concentrations of vapor (*i. e.*, high air mass fraction) in a vertical tube. They have shown that the condensation of small concentration of vapors is improved at lower wall temperature and the gas content causes a resistance to heat and mass transfer. Hassaninejadfarahani *et al.* [10] have developed a numerical analysis for laminar film condensation from high air mass fraction steam-air mixtures in vertical tube with constant wall temperature. They have used a finite volume method to the transformed equations resulting in a set of non-linear algebraic equations. Their results included radial direction profiles of axial velocity, temperature, air mass fraction as the axial variation of film thickness, Nusselt number, interface and bulk temperatures, interface and bulk air mass fraction, and proportion of latent heat transfer. Recently, a numerical study is presented by Zine-Dine *et al.* [11] in the case of laminar film condensation of a steam-gas mixture in the presence of non-condensable gas along a vertical tube wall subjected to a non-uniform heat flow. They have shown that the cooling of the wall tube by an external fluid is favorable to the process of condensation where it is more important for a larger convective heat transfer coefficient and a smaller cooling fluid temperature.

The purpose of the present work is to study the film condensation from a steam-air mixture. The conservation equations were used to determine the velocities, temperature, vapor mass fraction, and film thickness along the tube using the finite difference method. The first comparison is made with numerical studies of Hassaninejadfarahani *et al.* [10] and Merouani *et al.* [5]. The model is then compared with of Lebedev *et al.* [12], who performed an experimental study of the combined heat and mass transfer in vapor condensation from humid air. Hence, the present work focuses on the effects of non-condensable gas type in laminar film condensation from steam-gas mixture along a vertical tube wall subjected to a non-uniform heat flux.

Mathematical model

The geometry of the studied problem under consideration is a vertical tube with radius, R, length, L, and thickness, δ_z, which is very low compared to R, fig. 1. The tube wall, submitted to an external fluid (air), is then cooled by forced convection. A steam flow and non-condensable gas mixture are imposed at the entrance of the tube, with a uniform temperature, T_{in}, uniform velocity, u_{in}, uniform pressure, p_{in}, and vapor mass fraction, W_{in}. The following assumptions are adopted for the mathematical formulation.

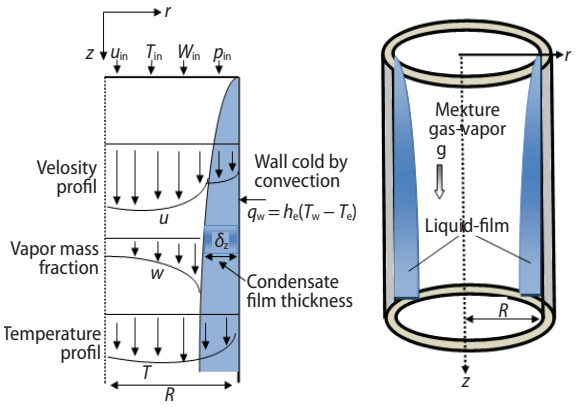

Figure 1. Physical model

– The flow is stationary, incompressible, laminar, bi-dimensional and axi-symmetric.
– Boundary-layer approximations are valid for both phases.
– Radiation heat transfer and viscous dissipation are negligible.
– The axial diffusion is negligible compared to convection.
– The gas-liquid interface is in the thermodynamic equilibrium, movable and without wave.
– The effect of the superficial tension of the liquid is negligible.

The governing equations corresponding to the conservation of mass, momentum, energy, diffusion, and the boundary conditions, in both gas and liquid phases are written for axisymmetric geometry:

– liquid film

$$\frac{\partial}{\partial z}\left(\rho_l u_l\right)+\frac{1}{r}\frac{\partial}{\partial r}\left(r\rho_l v_l\right)=0 \tag{1}$$

$$\frac{\partial}{\partial z}\left(\rho_l u_l^2\right)+\frac{1}{r}\left[\frac{\partial}{\partial r}\left(\rho_l r v_l u_l\right)\right]=-\frac{\mathrm{d}p}{\mathrm{d}z}+\frac{1}{r}\frac{\partial}{\partial r}\left(r\mu_l\frac{\partial u_l}{\partial r}\right)+\rho_l \mathrm{g} \tag{2}$$

$$\frac{\partial}{\partial z}\left(\rho_l C_p^l u_l T_l\right)+\frac{1}{r}\frac{\partial}{\partial r}\left(\rho C_p^l r v_l T_l\right)=\frac{1}{r}\frac{\partial}{\partial r}\left(r\lambda_l\frac{\partial T_l}{\partial r}\right) \tag{3}$$

– gas mixture

$$\frac{\partial}{\partial z}\left(\rho_m u_m\right)+\frac{1}{r}\frac{\partial}{\partial r}\left(r\rho_m v_m\right)=0 \tag{4}$$

$$\frac{\partial}{\partial z}\left(\rho_m u_m^2\right)+\frac{1}{r}\left[\frac{\partial}{\partial r}\left(\rho_m r v_m u_m\right)\right]=-\frac{\mathrm{d}p}{\mathrm{d}z}+\frac{1}{r}\frac{\partial}{\partial r}\left(r\mu_m\frac{\partial u_m}{\partial r}\right)+\rho_m \mathrm{g} \tag{5}$$

$$\frac{\partial}{\partial z}\left(\rho_m C_p^m u_m T_m\right)+\frac{1}{r}\frac{\partial}{\partial r}\left(\rho_m C_p^m r v_m T_m\right)=\frac{1}{r}\frac{\partial}{\partial r}\left(r\lambda_m\frac{\partial T_m}{\partial r}\right)+$$
$$+\frac{1}{r}\frac{\partial}{\partial r}\left[r\rho_m D\left(C_{p.\mathrm{v}}-C_{p.\mathrm{g}}\right)\right]\frac{\partial W}{\partial r}T_m \tag{6}$$

$$\frac{\partial}{\partial z}\left(\rho_m u_m W\right)+\frac{1}{r}\frac{\partial}{\partial r}\left(\rho_m r v_m W\right)=\frac{1}{r}\frac{\partial}{\partial r}\left(r\rho_m D\frac{\partial W}{\partial r}\right) \tag{7}$$

To complete the mathematical modeling of the problem, it is necessary to add the mass conservation equation in both gas and liquid phases, to the previous system.

– The global mass conservation equation is written:

$$\frac{\dot{m}_{\text{in}}}{2\pi} = \int_0^{R-\delta_z} r\rho_m u_m \mathrm{d}r + \int_{R-\delta_z}^{R} r\rho_l u_l \mathrm{d}r \tag{8}$$

Boundary and interface conditions

The imposed boundary and interface conditions are:

– condition at the inlet of the tube $z = 0$:

$$u_m = u_{\text{in}} \quad T_m = T_{\text{in}} \quad W = W_{\text{in}} \quad p_m = p_{\text{in}} \tag{9}$$

– condition on the central axis of the tube $r = 0$

– due to the symmetry:

$$\frac{\partial u_m}{\partial r} = 0 \quad \frac{\partial T_m}{\partial r} = 0 \quad \frac{\partial W}{\partial r} = 0 \quad v_m = 0 \tag{10}$$

– condition on the tube wall $r = R$:

$$u_l = v_l = 0 \tag{11}$$

The wall is cooled by convection with an external fluid at temperature T_e, the heat density is given by:

$$q_w = -\lambda_l \left.\frac{\partial T_l}{\partial r}\right|_w = h_e\left(T_w - T_e\right) \tag{12}$$

– Interfacial conditions $r = R - \delta_z$:

Continuities of the velocity and temperature (non-slip condition):

$$u_{\text{I}}(z) = u_{m,\text{I}} = u_{l,\text{I}} \quad T_{\text{I}}(z) = T_{m,\text{I}} = T_{l,\text{I}} \tag{13}$$

Continuities of the shear stress and heat flux:

$$\tau_{\text{I}} = \left(\mu\frac{\partial u}{\partial r}\right)_{l,\text{I}} = \left(\mu\frac{\partial u}{\partial r}\right)_{m,\text{I}} \tag{14}$$

The heat transfer at the interface can be generated by sensitive mode $Q_{\text{sen,I}}$ and latent mode $Q_{\text{Lat,I}}$ due to partial condensation of the liquid film. The total heat flow at the surface between the liquid phases to the gas phase is expressed:

$$Q_{\text{I}} = -\lambda_l \frac{\partial T_l}{\partial r} = -\lambda_m \frac{\partial T_m}{\partial r} + \dot{m}_{\text{I}} h_{\text{fg}} = Q_{\text{sen,I}} + Q_{\text{Lat,I}} \tag{15}$$

The mass flux exchanged between the two phases is given by Fick's law:

$$\dot{m}_{\text{I}} = -\rho_m D\left(\frac{\partial W}{\partial r}\right)_{\text{I}} \frac{1}{1 - W_{\text{I}}} \tag{16}$$

The mass fraction at the interface can be calculated using:

$$W_{\mathrm{I}} = \frac{p_{\mathrm{vs}} M_{\mathrm{v}}}{p_{\mathrm{vs}} M_{\mathrm{v}} + (p - p_{\mathrm{vs}}) M_{\mathrm{nc}}} \tag{17}$$

Characteristic variables

The local Nusselt and Sherwood numbers along the interface of gaseous mixture are defined by:

$$\mathrm{Nu}_z = \frac{h_t(2R)}{\lambda_m} = \frac{Q_{\mathrm{I}}(2R)}{\lambda_m (T_{\mathrm{b}} - T_{\mathrm{I}})} \quad \text{and} \quad \mathrm{Sh}_z = \frac{h_M(2R)}{D} = \frac{\dot{m}_{\mathrm{I}}(1 - W_{\mathrm{I}})(2R)}{\rho_m D(W_{\mathrm{b}} - W_{\mathrm{I}})} \tag{18}$$

With T_{b} and W_{b} are the bulk temperature and the bulk mass fraction of the mixture, respectively, which are given by the following expressions:

$$T_{\mathrm{b}} = \frac{\int_0^{R-\delta} \rho_m C_p^m r u_m T_m \mathrm{d}r}{\int_0^{R-\delta} \rho_m C_p^m r u_m \mathrm{d}r} \quad \text{and} \quad W_{\mathrm{b}} = \frac{\int_0^{R-\delta} \rho_m r u_m W \mathrm{d}r}{\int_0^{R-\delta} \rho_m r u_m \mathrm{d}r} \tag{19}$$

The total accumulated condensation rate is given by the expression:

$$M_{\mathrm{r}} = \frac{\text{condensate mass flow rate}}{\text{mass flow at the inlet}} = \frac{2\pi \int_0^z (R - \delta_z) \dot{m}_{\mathrm{I}} \mathrm{d}z}{\dot{m}_{\mathrm{in}}} \tag{20}$$

Numerical resolution method

Solution method

The conjugated nature of the problem leading to the parabolic system of eqs. (1)-(7) and appropriate boundary conditions makes it impossible to solve by any analytical method. Hence, the non-linear coupled differential equations of the system are solved by a finite difference numerical scheme. The axial convection terms are approximated by the backward difference while the transversal convection and diffusion terms are approximated by the central difference. Each system of the finite-difference equations forms a tridiagonal matrix equation, which can be solved by the Thomas algorithm in [13]. In the centerline ($r = 0$) of the tube, the diffusional terms are singular. A correct representation can be found from an application of L'Hospitals rule. In this study, the cylindrical co-ordinate r is transformed into η co-ordinate system, in such a way that the center line is at $\eta = 2$ the liquid-mixture interface is at $\eta = 1$ and the wall is at $\eta = 0$. The equations expressing η in terms of r are given by:

$$\begin{cases} \eta = 2 - \dfrac{r}{R - \delta_z} & \text{for} \quad 0 \le r \le R - \delta_z \\ \eta = \dfrac{R - r}{\delta_z} & \text{for} \quad R - \delta_z \le r \le R \end{cases} \tag{21}$$

Stability of the calculation scheme

Preliminary tests had been conducted to choose the accurate computational grid size. A non-uniform grid, based on geometrical progression in the axial and radial directions and

taking into account the irregular variation of u, W, and T at the gas-liquid interface and at the entrance, is then used. Hence, the density of the nodes is greater at the gas-liquid interface and at the tube entrance. Table 1 shows the variation of the local Nusselt and Sherwood numbers in terms of points in the axial direction (I) and the radial direction, respectively in the gas (J) and liquid (K). It is noted that the variations in the local Nusselt and Sherwood numbers, related to computations using grids ranging from 51 × (81+21) to 201 × (121+81), do not exceed 3%. In view of these results all further calculations were performed with the 131 × (81+31) grid.

Table 1. Comparisons of local interfacial Nusselt and Sherwood numbers for various grids along the tube (Re_{in} = 2000, p_{in} = 1 atm, T_{in} = 60 °C, and H_r = 50%)

		I × (J+K)				
z/*L*		51 × (81+21)	101 × (61+31)	131 × (81+31)	201 × (81+51)	201 × (121+81)
0.0470	Nu_z	21.69	21.30	20.70	20.75	20.81
	Sh_z	9.741	9.282	9.290	9.279	9.281
0.3498	Nu_z	13.70	13.71	13.70	13.70	13.69
	Sh_z	5.591	5.583	5.571	5.570	5.580
0.5559	Nu_z	12.30	12.31	12.30	12.30	12.30
	Sh_z	5.160	5.168	5.160	5.162	5.161
0.7531	Nu_z	11.35	11.39	11.36	11.39	11.40
	Sh_z	4.952	4.965	4.950	4.96	4.96
1.00	Nu_z	10.51	10.53	10.51	10.54	10.55
	Sh_z	4.801	4.815	4.808	4.818	4.818

Validation of numerical code

In order to verify the accuracy of the present numerical code, the obtained results are compared to those reported by Hassaninejadfarahani *et al.* [10] and Merouani *et al.* [5] in the case of laminar condensation of a steam-air in a vertical tube with a wall maintained at temperature T_w = 5 °C. The results have been also compared with the experimental data results presented by Lebedev *et al.* [12].

The first comparison is presented in fig. 2, which illustrate the evolution of the air mass fraction, fig. 2(a), and dimensionless bulk temperature, fig. 2(b) at various axis, for an inlet pressure p_{in}=1 bar, T_{in} = 40 °C, H_r = 100%, L = 1 m, and R = 12.5 mm. The variation of 1 – W

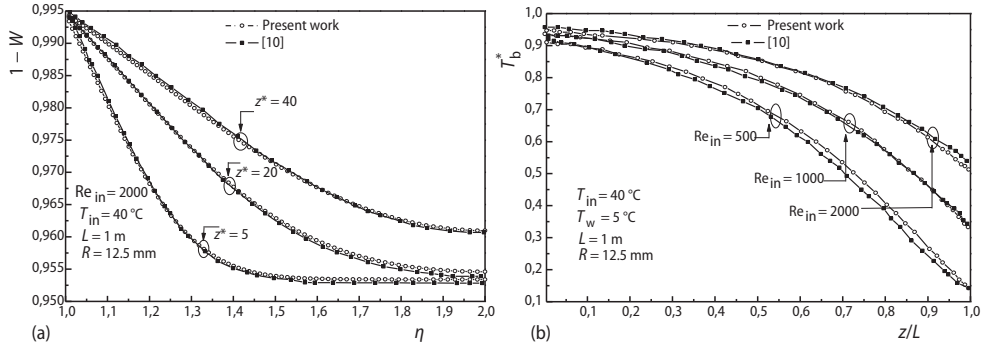

Figure 2. Comparison of air mass fraction (a) and bulk temperature (b) with Hassaninejadfarahani *et al.* [10]

in fig. 2(a) shows that near the inlet ($z^* = 5$), the air mass fraction is equal to $1 - W_{in}$ for most of the cross-sections and the non-condensable gas increases rapidly near the interface because of the adopted interface impermeability condition. In fig. 2(b), the bulk temperature T^*_b decreases along the axial direction and increases with the increase of Reynolds number. A good agreement is then observed between the present study and Hassaninejadfarahani *et al.* [10]. In fact, the relative gap does not exceed 1.2% in fig. 2(a) and 6% in fig. 2(b). This difference is due to the different used method (implicit finite difference method and finite volume method), to the type of correlations and to the thermophysical properties.

The second comparison is based on the experimental data of Lebedev *et al.* [12] in the case of heat and mass transfer in vapor condensation from humid air along a rectangular channel with 0.02 m wide, 0.15 m high, 0.6 m long, inlet temperature 60 °C, inlet pressure 1.01325 bar, and relative humidity 100%. Figure 3(a) presents the local condensate heat transfer coefficient $h_{l,z}$ for different values of mixtures content (gm water vapor per kg dry air). From this figure, and for two different velocities at the inlet, $u_{in} = 1.4$ m/s ($Re_{in} = 1480$) and $u_{in} = 0.7$ m/s ($Re_{in} = 740$). To compare the present numerical results with those of Lebedev *et al.* [12] at the same conditions concerning the inlet Reynolds number, inlet temperature and inlet pressure, we use other data defined by: $H_r = 100\%$, $p_{in} = 1.01325$ bar, $L = 0.6$ m, and $d_e = 0.02$ m, where d_e is the hydraulic diameter equivalent in the case of the duct. It is apparent that the results obtained from the present work are in good concordance with those of Merouani *et al.* [5] and the experimental study of Lebedev *et al.* [12]. We have also compared the variation of average Nusselt number of sensible heat for different inlet Reynolds number fig. 3(b). It finds that the agreement is satisfactory between this study and the references [5, 10, 12].

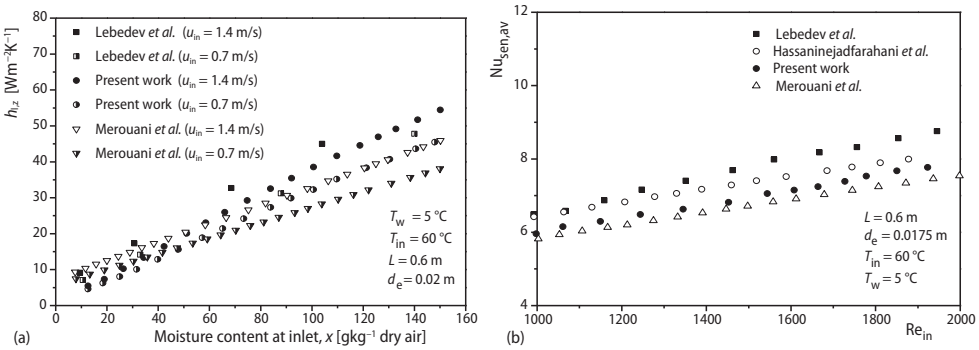

Figure 3. Comparison of a local condensate heat transfer coefficient $h_{l,z}$ (a) and average Nusselt number of sensible heat $Nu_{sen,av}$ (b) with [5, 10, 12]

Results and discussion

In this study, calculations are performed specifically with four non-condensable gases krypton, argon, air, and neon during condensation of water vapor inside a vertical tube with length $L = 2$ m, diameter $D = 2$ cm, and under the following operating requirements: inlet vapor mass fraction $W_{in} = 0.8$, temperature difference between inlet vapor gas mixture and cooling fluid $\Delta T = T_{in} - T_e = 20$ °C, inlet Reynolds number $Re_{in} = 2000$ and inlet pressure $p_{in} = 1$ atm. The gas-steam mixture is saturated (relative humidity $H_r = 100\%$), the wall is cooled by air-flow at temperature T_e. The study is performed to examine the effect of non-condensable gas type.

In order to analyze the heat and mass transfer between the liquid phase and the vapor one, figs. 4(a) and 4(b) illustrate, respectively, the temperature profiles on wall and in the

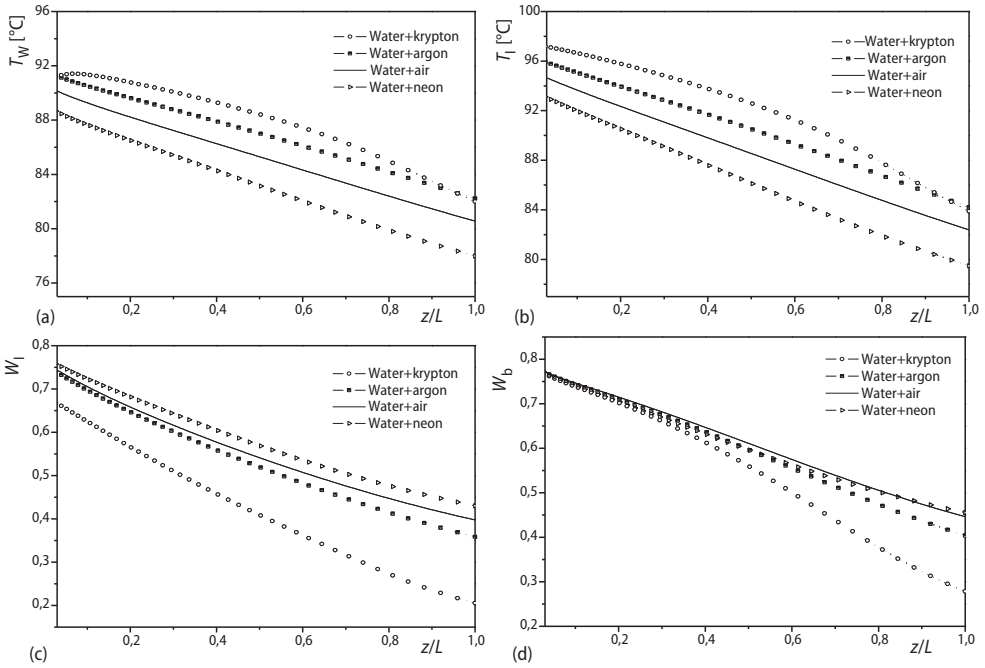

Figure 4. Axial variation of wall temperature (a), interface temperature (b), interface mass fraction (c), and bulk mass fraction (d) along the tube for different non-condensable gases

interface for different non-condensable gases. It is observed that for constant p_{in}, W_{in}, and ΔT, the wall and interface temperatures in the water vapor-krypton mixture are significantly higher and those of the water-neon mixture are less important compared to the other mixtures. This is explained by the increase of the molar mass of non-condensable gas which causes an increase in the density of gas mixture and consequently an increase of saturation pressure and saturation temperature of mixture which are promoting the condensation. In addition, it is found that the wall and interface temperatures decrease sharply along the tube and tend asymptotically towards the cooling fluid temperature, this decrease results from the energy expended to condensation and indicates that the energy required to support the condensation has to come from the internal energy of the liquid film.

The influence of the type of non-condensable gas on the axial interface and bulk vapor mass fraction along the tube is illustrated in figs. 4(c) and 4(d), it is found that the interface vapor mass fraction fig. 4(c) decreases along the tube for all non-condensable gas and varies in the same way as the interface temperature fig. 4(b). This variation is due to the thermodynamic equilibrium at the interface between the gas phase and the liquid one. It is also observed that for the water-neon mixture having a lower mass density, its interface and bulk mass fractions are the highest. This is due to the increasing of saturation pressure which results from an increase of saturation temperature.

Figures 5(a) and 5(b) represents, respectively, the variation of interfacial mass condensation rate and liquid film thickness along the tube for the four different non-condensable gases (neon, air, argon, and krypton). The condensation mass flux decreases very rapidly to 0 for all steam-gas mixtures, which means the end of the condensation. It is noted that the condensation mass flux and the film thickness of water krypton mixture, which is the heaviest

(high molar mass), are the highest ones compared to the other gas mixtures. This means that the increase of the mass density and the decrease of the diffusion coefficient of the gas mixture cause an increase in the Schmidt number characterizing the flow of gaseous mixture.

The total transferred heat is resulting from two phenomena: the temperature difference between the wet mixture and the interface causing a sensible heat transfer and the condensation of steam at the interface providing a latent heat. Figures 5(c) and 5(d) show, respectively, the effect of non-condensable gas type on the latent and sensible heat fluxes along the tube. Note that the latent and sensible heat fluxes decrease along the tube. This implies that the steam will lose the latent heat by condensation, it also loses sensible heat due to the decrease of temperature mixtures. Moreover, among the four mixtures mentioned above the heat transfer by latent, fig. 5(c) and sensible, fig. 5(d) modes are more important in the case of water-krypton mixture particularly near the entrance edge of the tube where the temperature and the vapor concentration gradients are greatest. This is confirmed by fig. 5(a).

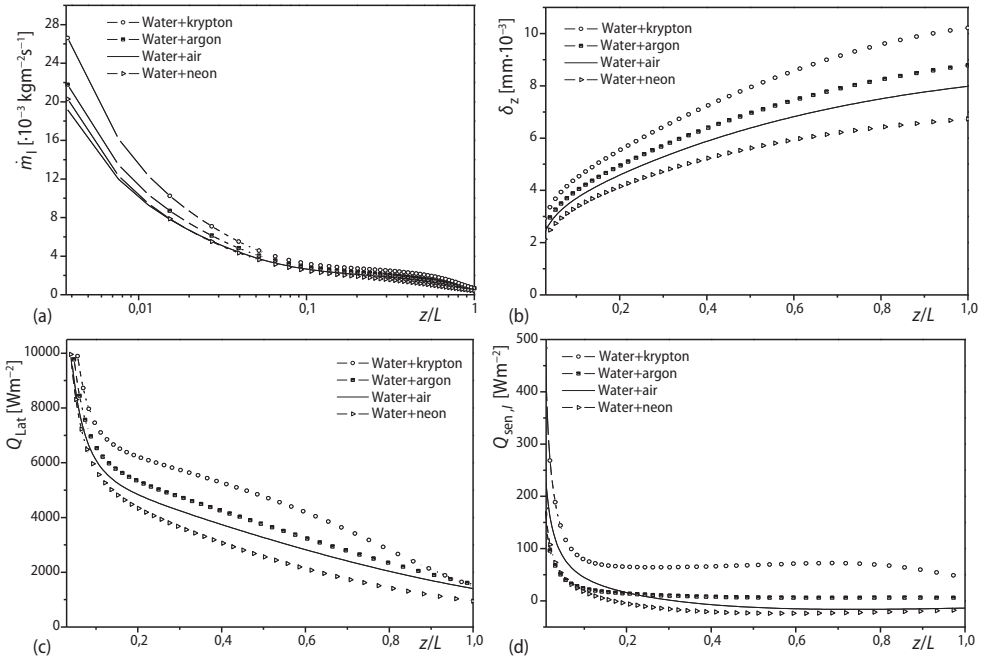

Figure 5. Axial variation of interfacial mass condensation rate (a), liquid film thickness (b), latent heat flux (c), and sensible heat flux (d) along the tube for different non-condensable gases

Distribution of dimensionless vapor mass fraction for different sections of the tube is shown in fig. 6(a). The water vapor mass fraction increases from the interface toward the center of the tube and also decreases from the inlet to the outlet of tube where it becomes almost constant. Increasing the molar mass of the gas causes a decrease in the final saturations concentration, especially for the krypton-steam mixture which has the lowest concentration as confirmed by fig. 4.

Figure 6(b) shows the variation of dimensionless velocity of steam for different sections of the tube. Moving away from the tube inlet and with increasing of z^*, it is found that the mixture velocity decreases from the symmetry axis of the tube to approach a value of the liquid phase at the liquid vapor interface. In the liquid phase, the velocity profiles continue to

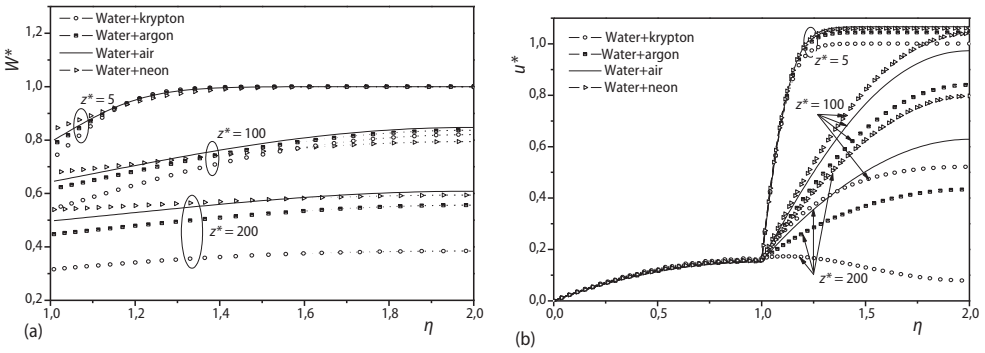

Figure 6. Variation of dimensionless vapor mass fraction (a) and dimensionless vapor velocity (b) for different non-condensable gases

decrease until the tube wall, where they become almost independent of z^* and confounded for the four non-condensable gas. This trend is due to the mass transfer from the mixture toward the liquid film. A boundary-layer appears from the mixing zone to the liquid vapor interface, with a thickness increasing with z^*. We also observe that the steam velocity in the presence of non-condensable gas krypton is lower compared to the other three gas mixtures as confirmed by fig. 6(a).

In order to better understanding of the relative importance of latent and sensible heat transfer, figs. 7(a) and 7(b) present the evolution of reduced quantities (Q_{Lat}/q_w, Q_{sen}/q_w) exchanged along the tube for different steam-gas mixture. It is found that the relative latent and sensible heat flux are higher for water vapor-krypton. This can be explained by the increase in

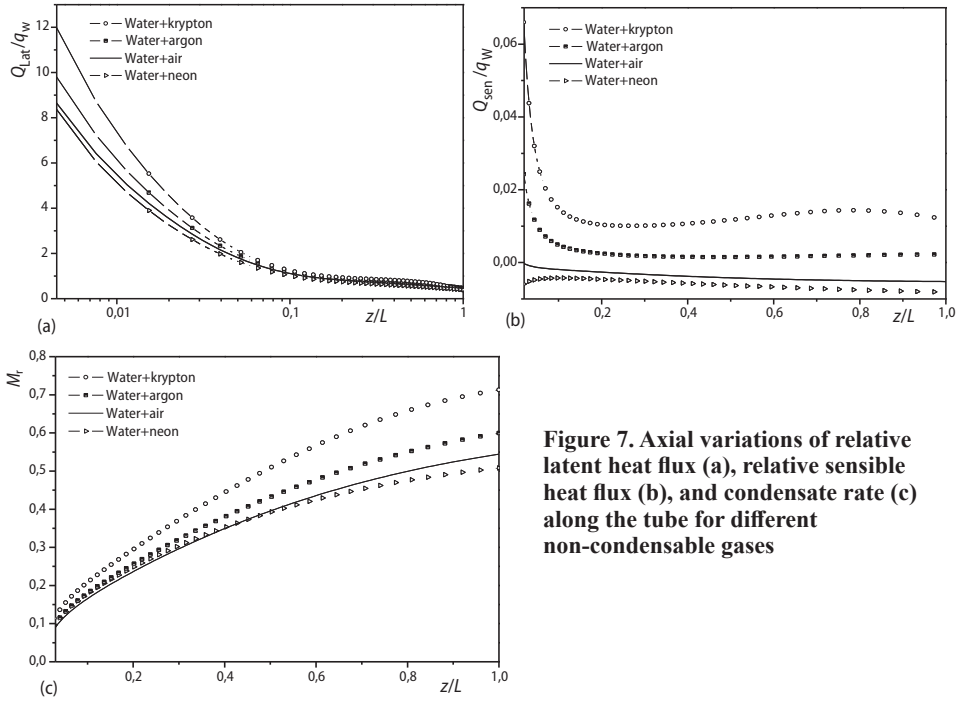

Figure 7. Axial variations of relative latent heat flux (a), relative sensible heat flux (b), and condensate rate (c) along the tube for different non-condensable gases

the latent and sensible heat flow and therefore a decrease of relative latent and sensible heat flux. The evolution of condensate rate increases along the tube for all gas mixtures fig. 7(c), and it is higher in the case of water-krypton mixture. According to these results the condensate rate can be classified in ascending order of the molar mass of non-condensable gas as: neon, air, argon and krypton.

Conclusions

A numerical analysis has been carried out to investigate the effect of non-condensable gas type in low mass fraction during condensation of water steam inside a vertical tube with wall cooled by air-flow. Governing equations are solved using an implicit finite difference scheme. Results have been obtained for steam-gas mixtures for given sets of the governing parameters imposed at the inlet of the tube and on the wall, such as: pressure, Reynolds number, temperature, and mass fraction. Based on the numerical results, the main conclusions are as follows.

- The non-condensable gas type plays an important role on the intensity of heat and mass transfer occurring between the two phases.
- An increase of the molar mass of gas leads on one hand to the enhancement of the mixture density, its saturation temperature and the wall temperature, and on the other hand to the decrease of the saturated vapor concentration. Therefore, the heaviest mixture (steam-krypton) presents the lowest vapor mass fraction in the tube exit.
- The liquid film thickness, the condensation mass flux, the condensate rate and the latent and sensible heat fluxes at the tube inlet are higher when the molar mass of non-condensable gas is higher and therefore there is an increase of the gas mixture density.
- The gaseous mixtures with high Schmidt number, is subjected to a significant accumulation of gas at the interface and consequently, leads to a larger condensation process.

Nomenclature

C_p – specific heat, [Jkg^{-1}K^{-1}]
D_m – diffusion coefficient, [m^{2}s^{-1}]
D – diameter of tube (= 2R), [m]
g – gravity acceleration, [ms^{-2}]
H_r – relative humidity, [%]
h_{fg} – latent heat of vaporization, [Jkg^{-1}]
h_e – coefficient of external convection fluid-wall, [Wm^{-2}K^{-1}]
h_M – masse transfer coefficient, [ms^{-1}]
h_t – heat transfer coefficient, [Wm^{-2} K^{-1}]
L – length of tube, [m]
M_{nc} – molar mass of non-condensable gas, [kg kmol^{-1}]
M_r – condensate mass rate, [–]
M_v – molar mass of water vapor, [kg kmol^{-1}]
$\dot{m}_{in}$ – gas mass flow, [kgm^{-2}s^{-1}]
$\dot{m}_I$ – mass flux at the interface, [kgm^{-2}s^{-1}]
Nu_z – local Nusselt number, [–]
P – mixture pressure, [Pa]
p_{in} – mixture pressure, [bar]
Q_I – total heat flux, [Wm^{-2}]
Q_{Lat} – latent heat flux, [Wm^{-2}]
Q_{sen} – sensible heat flux, [Wm^{-2}]
q_w – heat flow to wall, [Wm^{-2}]
R – radius of tube, [m]
Re_{in} – inlet Reynolds number, (= 2$Rp_{in}u_{in}/m_{in}$)
r – radial co-ordinate, [m]
Sh_z – local Sherwood number
T – dimensional temperature, [K]
T_e – external fluid temperature, [K]
T^* – dimensionless temperature, [= ($T - T_w$)/($T_{in} - T_w$)], [–]
T_w – wall temperature, [K]
ΔT – difference temperature (= $T_{in} - T_e$), [K]
u – velocity in the z-direction, [ms^{-1}]
u^* – dimensionless velocity in the z-direction (= u/u_{in})
v – velocity in the r-direction, [ms^{-1}]
W – vapor mass fraction
W^* – dimensionless vapor mass fraction, (= W/W_{in}), [–]
z – axial co-ordinate, [m]
z^* – dimensionless axial co-ordinate, (= $z/2R$), [–]

Greek symbols

δ – condensate film thickness, [m]
η – dimensionless radial co-ordinate, [–]
λ – thermal conductivity, [Wm^{-1}K^{-1}]
μ – dynamic viscosity, [kgm^{-1}s^{-1}]
ρ – density, [kgm^{-3}]

Subscripts

av – average
b – bulk
e – extern
g – gas
I – interface liquid-gas
in – at the tube inlet
Lat – latent
l – liquid film
m – mixture
nc – non-condensable gas
sen – sensible
v – vapor
vs – saturated vapor

References

[1] Nusselt, W., The Condensation of Steam on Cooled Surfaces, *Zeitschrift des Vereines Deutscher Ingenieure*, *60* (1916), 27, pp. 541-575
[2] Rohsenow, W. M., Heat Transfer and Temperature Distribution in Laminar Film Condensation, *Trans. ASME., 78* (1956), 1956-1648
[3] Siddique, M., *et al.*, Local Heat Transfer Coefficients for Forced-Convection Condensation of Steam in a Vertical Tube in the Presence of Noncondensable Gas, *Nuclear Technology, 102* (1993), 3, pp. 386-402
[4] Siddique, M., *et al.*, Theoretical Modelling of Forced-Convection Condensation of Steam in a Vertical Tube in the Presence of a Noncondensable Gas, *Nuclear Technology, 106* (1994), May, pp. 202-215
[5] Merouani, L., *et al.*, Numerical Modelling of Convective Vapour Condensation with Non-Condensable Gases between Two Coaxial Vertical Cylinders, *The Canadian Journal of Chemical Engineering. 91* (2013), 9, pp.1597-1607
[6] Maheshwari, N. K., *et al.*, Investigation on Condensation in Presence of a Noncondensable Gas for a Wide Range of Reynolds Number, *Nuclear Engineering and Design, 227* (2004), 2, pp. 219-238
[7] Oh, S., Revankar, S. T., Effect of Noncondensable Gas in a Vertical Tube Condenser, *Nuclear Engineering and Design, 235* (2005), 16, pp. 1699-1712
[8] Saffari, H., Dalir, N., Effect of Virtual Mass Force on Prediction of Pressure Changes in Condensing Tubes, *Thermal Science, 16* (2012), 2, pp. 613-622
[9] El Hammami, Y., *et al.*, Numerical Study of Condensing a Small Concentration of Vapour Inside a Vertical Tube, *Heat and Mass Transfer, 48* (2012), 9, pp. 1675-1685
[10] Hassaninejadfarahani, F., *et al.*, Numerical Analysis of Mixed Convection Laminar Film Condensation from High Air Mass Fraction Steam – Air Mixtures in Vertical Tubes, *International Journal of Heat and Mass Transfer, 78* (2014), Nov., pp. 170-180
[11] Zine-Dine, K., *et al.*, Numerical Study of Laminar Film Condensation inside a Vertical Tube Subjected to Wall Non-Uniform Heat Flux, *International Journal of Enhanced Research in Science, Technology & Engineering, 5* (2016), 2, pp. 168-180
[12] Lebedev, P. D., *et al.*, Aerodynamics Heat and Mass Transfer in Vapour Condensation from Humid Air on a Flat Plate in a Longitudinal Flow in Asymmetrically Cooled Slot, *Int. J. Heat Mass Transf., 12* (1969), 8, pp. 833-841
[13] Patankar, S. V., *Numerical Heat Transfer and Fluid Flow*, Hemisphere/Mc Graw-Hill, New York, USA, 1980, Chap. 6

Paper submitted: June 12, 2016
Paper revised: November 2, 2016
Paper accepted: November 7, 2016